Statistical Monitoring of the Hand, Foot and Mouth Disease in China

Jingnan Zhang

Department of Biostatistics, University of Florida, Gainesville, 32611, USA

**email:* zhan1441@ufl.edu

and

Yicheng Kang

Department of Biostatistics, University of Florida, Gainesville, 32611, USA

**email:* kangx276@ufl.edu

and

Yang Yang

Department of Biostatistics, University of Florida, Gainesville, 32611, USA

**email:* yangyang@ufl.edu

and

Peihua Qiu

Department of Biostatistics, University of Florida, Gainesville, 32611, USA

**email:* pqiu@ufl.edu

SUMMARY: In a period starting around 2007, the Hand, Foot and Mouth Disease (HFMD) became wide-spreading in China, and the Chinese public health was seriously threatened. To prevent the outbreak of infectious diseases like HFMD, effective disease surveillance systems would be especially helpful to give signals of disease outbreaks as early as possible. Statistical process control (SPC) charts provide a major statistical tool in industrial quality control for detecting product defectives in a timely manner. In recent years, SPC charts have been used for disease surveillance. However, disease surveillance data often have much more complicated structures, compared to the data collected from industrial production lines. Major challenges, including lack of in-control data, complex seasonal effects, and spatio-temporal correlations, make the surveillance data difficult to handle. In this paper, we propose a three-step procedure for analyzing disease surveillance data, and our procedure is demonstrated using the HFMD data collected during 2008-2009 in China. Our method uses nonparametric longitudinal data and time series analysis methods to eliminate the possible impact of seasonality and temporal correlation before the disease incidence data are sequentially monitored by a SPC chart. At both national and provincial levels, our proposed method can effectively detect the increasing trend of disease incidence rate before the disease becomes wide-spreading.

Key words: ARIMA model; Bootstrap; Disease surveillance and prevention; Early detection; Nonparametric longitudinal data analysis; Statistical process control; Time series.

1. Introduction

The Hand, Foot and Mouth Disease (HFMD) is a common infectious disease caused by a group of non-polio enteroviruses that belongs to the Human Enterovirus species A (HEV-A). Its main clinical symptoms include a brief prodromal fever followed by pharyngitis, mouth ulcers and rash on the hands and feet. In most cases, the disease is mild and self-limiting. However, severe clinical complications with neurological symptoms, such as meningitis, encephalitis and polio-like paralysis, may occur (cf., Wang et al., 2011). In 2009, the number of HFMD cases reported in mainland China amounted to 1,155,525, including 13,810 (or 1.2%) severe cases and 353 (or 0.03%) deaths. The high case-fatality rate was attributed to reasons such as the rapid disease progression, late clinical treatment, and limited local medical capacity. It was also found that the case-fatality rate decreased considerably once the early clinical treatment was provided to patients with severe symptoms. Therefore, effective disease surveillance and timely implementation of disease prevention and control measures are critically important for minimizing the damage of HFMD (cf., World Health Organization, 2011). This paper presents a case study of the HFMD data collected in China during 2008-2009. It will show that certain statistical methods are helpful in early detection of the HFMD outbreaks.

In the statistical literature, statistical process control (SPC) charts provide a major statistical tool for monitoring industrial production lines and for controlling product quality (cf., Qiu, 2014). In recent several years, SPC charts have been frequently used for disease surveillance and prevention (cf., Woodall, 2006). In this regard, some authors model the number of disease incidents by a Poisson distribution and construct likelihood-ratio-based control charts for disease monitoring (Zhou and Lawson, 2008). Some people develop control charts based on parametric time series modeling of the possible temporal correlation in the observed data (Watier, Richardson and Hubert, 1991). Some others propose multivariate control charts to accommodate the spatial pattern exhibited by surveillance data (e.g., Jiang et al., 2011, Rogerson and Yamada, 2004). However, disease surveillance data often have much more complicated structures, compared to the data collected from industrial production lines. Many issues about the observed disease incidence data need to be carefully addressed before an SPC chart can be applied. For example, the Poisson distribution model and other parametric distribution models are rarely valid in practice. The disease incidence often has a complicated seasonal trend, and the conventional SPC chart cannot handle such a trend properly. It is critically important to address all such issues properly in order to effectively detect the HFMD outbreaks.

In this paper, we propose a three-step procedure for detecting HFMD outbreaks, and this procedure is demonstrated using the HFMD data collected by the Chinese CDC during 2008–2009. Our proposed method consists of the following three steps:

(i) *Detrend* – Seasonality in the disease incidence data is first described by a nonparametric longitudinal model, and is then eliminated from the observed data,

(ii) *Decorrelation* – Temporal autocorrelation in the detrended data is modeled by an ARIMA model, and is then eliminated from the detrended data, and

(iii) *Sequential Monitoring* – The detrended and decorrelated data obtained in step (ii) are then sequentially monitored by an SPC chart.

The remainder of this article is organized as follows. In Section 2, the HFMD data and the proposed three-step procedure are described in more details, and the results of our analysis of the HFMD data at the national level are also presented there. In Section 3, results of our analysis for individual provinces are presented, and a data-driven procedure for searching for the control limit of the SPC chart is discussed as well. Several remarks conclude the article in Section 4.

2. Nationwide Monitoring of HFMD

The data used in our analysis were collected by the HFMD reporting system in China from December 2008 to November 2009. The system recorded the reporting times of diagnosed HFMD cases and the locations of the reporting clinics nationwide in real time. Locations of the reporting clinics were registered in the format of administrative code that consists of 6 digits. Based on this code, we can identify administrative divisions of the country at the village level and above. In this section, we combine the observed data of different administrative divisions in the nation for monitoring HFMD at the national level. The national HFMD incidences in China during December 2008 and November 2009 are shown in Figure 1. To monitor this data properly, we need to take into account the seasonal trend and the temporal correlation in the data before applying a control chart for sequential monitoring. The reason is that conventional control charts are based on the assumptions that process observations have a constant mean and a constant variance when the process is in-control (IC) and that they are independent of each other across different obvervation times. In cases when these assumptions are violated, it has been well demonstrated in the literature that the control charts are not reliable (cf., Qiu, 2014, Chapters 4 and 5). For instance, if there is a seasonal trend in the data and it is not removed beforehand, then the seasonal trend can trigger a signal of the control chart, and consequently we cannot distinguish signals due to HFMD outbreaks from those due to seasonality in the data. Similarly, it has been well demonstrated that the temporal correlation can delay or hasten the signal of a control chart and therefore they need to be addressed properly for a reliable process monitoring (cf., Maragah and Woodall, 1992, Montgomery et al., 1991). In the next three subsections, we will address all these issues and describe the proposed three-step procedure in details.

[Figure 1 about here.]

2.1 *Baseline Seasonal Trend*

Like other infectious diseases, incidence of HFMD fluctuates over time and exhibits obvious seasonal variation (Wang et al., 2011). Usually, such seasonal variation is not the main interest of disease surveillance. In this subsection, we try to describe the seasonal variation using a statistical model, and then remove it from the observed data for subsequent data analysis. Ideally, the seasonal variation should be estimated from the observed data collected in years when no disease outbreaks are present. Such data are called baseline data in this paper. Unfortunately, Chinese government did not have a formal reporting system for collecting HFMD incidence data before the outbreak took place in 2008. The lack of such baseline data makes it challenging to accurately estimate the seasonal effect. However, with the collected data at the provincial level, the following fact can be noticed. While densely populated metropolitan areas (e.g., Beijing, Shanghai, etc.) were affected by HFMD seriously during 2008-2009, the HFMD incident rates (defined to be the ratios of the numbers of reported HFMD cases to the populations of the individual provinces) remain relatively stable in some remote provinces. Thus, it is reasonable to use the data recorded in those remote provinces to fit the baseline model. It should be pointed out that the incident rate instead of the disease count is used here because different provinces have quite different populations and the incident rate can adjust for the population properly.

To determine which province can be included in the baseline data, we use the following criterion. For each province, its daily incident rates are calculated by dividing the daily HFMD counts by its population. Then, the highest daily incident rate is obtained. If the highest daily incident rate is below a threshold value, then that province is assumed to have no HFMD outbreaks in the entire period of observation and that province can be included in the baseline data. In this procedure, the population data of various provinces are obtained from the official website of Chinese Census Bureau. Bie et al. (2010) estimated the average incidence rate of HFMD in China to be 0.0037 per 1,000 people in regular years when no HFMD outbreaks exist. Therefore, we choose 0.0037 as the threshold value mentioned above, based on which the following five provinces are included in the baseline data: Guizhou, Xinjiang, Sichuan, Yunnan, and Tibet. Then, the average daily HFMD incidence rates of the five provinces are computed and they are denoted as r_t with t being the time. Assume that r_t follows the nonparametric regression model

$$r_t = f(t) + \varepsilon_t, \qquad \text{for } t = 1, 2, \ldots, n, \tag{1}$$

where $f(t)$ is a real-valued continuous function of t denoting the mean of r_t, ε_t is the mean-0 error term, and $n = 365$ is the number of observations in the baseline data. Then, $f(t)$ can be used for describing the *seasonal effect*. The local quadratic kernel smoothing method (cf., Chapter 2, Qiu, 2005) is used for estimating $f(t)$, in which the conventional Epanechnikov kernel function is used and the bandwidth is chosen by the 10-fold cross-validation (CV) procedure. The estimated $f(t)$, denoted as $\widehat{f}(t)$, is shown in Figure 2 by the solid curve, with the baseline data shown by the little circles. From the figure, we can see an obvious seasonal pattern that the HFMD incidence is high in late spring and early summer, relatively low in the autumn, and low in the winter. It should be pointed out that the autocorrelation is not taken into account in this analysis for simplicity. The estimator $\widehat{f}(t)$ can be regarded as the local linear generalized estimating equations (GEE) estimator discussed in Lin and Carroll (2000). The GEE estimator can accommodate autocorrelation without specifying the autocorrelation structure by using the so-called independent working correlation matrix. Under certain mild conditions, Lin and Carroll have shown that it is asymptotically the best estimator. Therefore, $\widehat{f}(t)$ should be an efficient estimator of $f(t)$.

[Figure 2 about here.]

2.2 *Temporal Correlation*

Let Z_t be the national daily counts of HFMD. Define

$$Y_t = Z_t - \widehat{f}(t) M_t, \qquad \text{for } t = 1, 2, \ldots, n, \tag{2}$$

where $\widehat{f}(t)$ is the estimated baseline incidence rate obtained from model (1), and M_t is the national population at time t. Then, $\{Y_t : t = 1, 2, \ldots, n\}$ can be interpreted as the daily counts of HFMD after the seasonal trend is removed. The quantities Z_t and $\widehat{f}(t)M_t$ are shown in Figure 3(a) by the solid and dashed curves, respectively. It can be seen from the plot that the national seasonal trend has been captured reasonably well by the estimated baseline model (1) discussed in the previous subsection. The detrended data $\{Y_t : t = 1, 2, \ldots, n\}$ are shown in Figure 3(b) where the vertical dashed line separates the first 80 observations from the remaining ones. From the plot, it can be seen that Y_t remains quite stable when $1 \leqslant t \leqslant 80$ (i.e., Dec 1 - Feb 18, 2009).

[Figure 3 about here.]

Sequential monitoring of a process is often divided into two phases (cf., Chapter 1, Qiu, 2014). In phase I, the distribution of the process observations in the case when the process is IC, i.e., no disease outbreaks are present in the current setup, can be estimated from an IC dataset. Then, the online sequential monitoring of the process is executed in phase II. For the data shown in Figure 3(b), the first 80 observations $\{Y_t, t = 1, \cdots, 80\}$ can be assumed to be an IC dataset, and we start to online monitor the sequence at the 81st time point. For the detrended data, temporal correlation might exist. As mentioned earlier, in the SPC literature, conventional control charts assume that observations are independent of each other, and the temporal correlation needs to be properly addressed for a reliable process monitoring.

Next, we try to use a time series model to describe the temporal correlation in the IC data. In the time series literature, the popular and flexible time series model is the

ARIMA (p,d,q) model (Box and Jenkins, 1976), where p, d, and q are three parameters, p is the order of autoregression, q is the the order of moving average, and d is the order of difference (see Shumway and Stoffer (2011) for their mathematical definitions). To estimate the ARIMA model, we suggest selecting d using the successive KPSS unit-root test proposed by Kwiatkowski et al. (1992) to determine the number of differences required for the time series model to be stationary. The KPSS test is for testing the the null hypothesis that the time series model is stationary. It proceeds as follows. First, a unit-root test (Dickey and Fuller, 1979) is applied to $\{Y_t : t = 1, 2, \ldots, 80\}$ to test whether the time series is stationary using an autoregressive model. If the p-value of this test is smaller than a pre-specified significance level α, then we proceed to run the unit-root test again on the first-order differenced data $\{Y_{t+1} - Y_t, t = 1, 2, \ldots, 80\}$. If the p-value is once again smaller than α, then we continue to run the test on the second-order differenced data. This process continues until obtaining the first insignificant p-value (i.e., p-value is bigger than or equal to α). Throughout this paper, if no further specification, α is fixed at 0.05. Once d is determined, p and q are chosen by minimizing some model selection criterion. Kwiatkowski et al. (1992) suggested using the AICc criterion for selecting p and q, which is adopted in this paper.

After implementing the model estimation procedure described above, we choose the following ARIMA(1, 1, 0) model:

$$Y_{t+2} - Y_{t+1} = \phi \ (Y_{t+1} - Y_t) + w_t, \text{ for } t = 1, 2, \ldots, 80, \tag{3}$$

where w_t's are the i.i.d. random errors with mean 0 and unknown variance $\sigma_w^2 > 0$. The estimated value of ϕ is $\widehat{\phi} = 0.22$. The standardized residuals of the fitted model (3) is shown in Figure 4(a). If the model is appropriate, the residuals should look like the white noise from a distribution with mean 0. One way to assess whether this is true is to perform the Ljung-Box test (cf., Shumway and Stoffer, 2011). The p-value of the of Box-Ljung test in the current case is 0.23, which indicates that the autocorrelation in $\{Y_t : t = 1, 2, \ldots, 80\}$ has been described well by (3) and there is no significant autocorrelation among the residuals of the estimated model (3). The density histogram of the residuals shown in Figure 4(a), the corresponding estimated density curve (solid line), and the density curve of the normal distribution with the same mean and variance (dashed line) are shown in Figure 4(b). From the plot, the distribution of the residuals is close to normal. As a matter of fact, the Shapiro-Wilk normality test gives a p-value of 0.4413, which confirms that the distribution of the residuals is not significantly different from normal.

[Figure 4 about here.]

2.3 *Sequential Monitoring*

After model (3) is estimated, the estimated model can be applied to the phase II detrended data $\{Y_t : t = 81, 82, \ldots, n\}$ to obtain the detrended and decorrelated phase II data $\{\widehat{w}_t = (Y_{t+2} - Y_{t+1}) - \widehat{\phi}(Y_{t+1} - Y_t),\ t = 81, 82, \ldots, n-2\}$. If no HFMD outbreaks exist, then these data should roughly follow a normal distribution with mean 0. Otherwise, the outbreaks will be reflected in the mean shifts of $\{\widehat{w}_t,\ t = 81, 82, \ldots, n-2\}$, as demonstrated by several papers, including Jiang et al. (2000), Lu and Reynolds (2001), and Williamson and Hudson (1999). Therefore, to detect the HFMD outbreaks, we can simply monitor the detrended and decorrelated phase II data $\{\widehat{w}_t,\ t = 81, 82, \ldots, n-2\}$. To this end, it has been well justified that SPC charts (e.g., the Shewhart, CUSUM and EWMA charts) are effective tools (cf., Qiu, 2014). Because it has been justified that the IC distribution of $\{\widehat{w}_t,\ t = 81, 82, \ldots, n-2\}$ is close to a normal distribution and we are mainly concerned about upward shifts in the HFMD incidence rates, we can consider using the classical CUSUM chart with the charting statistic

$$C_t = \max\left(0, C_{t-1} + \widehat{w}_t - k\right), \tag{4}$$

where $C_0 = 0$, and $k > 0$ is an *allowance* constant. The chart gives a signal of an upward mean shift when

$$C_t > h,$$

where $h > 0$ is a *control limit*. In the SPC literature, k is usually chosen beforehand. It has been well demonstrated that a larger k is good for detecting a larger shift, and a smaller k is good for detecting a smaller shift. The chart (4) with a given k value, say k_0, is optimal for detecting the shift of size $2k_0$ in the sense that its out-of-control (OC) average run length (ARL) is the shortest among all control charts with a given IC ARL value (Moustakides, 2004). Here, the IC ARL value is defined to be the average number of time points from the beginning of process monitoring to the signal time when the process is IC, and the OC ARL value is defined to be the average number of time points from the occurrence of a shift to the signal time after the process becomes OC (cf., Section 4.2, Qiu, 2014). Therefore, the concepts of the IC and OC ARL values are similar to the type-I error probability and power in the hypothesis testing context. In practice, the IC ARL value is often specified beforehand, and then a chart performs better if its OC ARL value is smaller when detecting a shift of a given size. Commonly used IC ARL values include 100, 200, 370, 500, and 1000.

Next, we consider two commonly used IC ARL (denoted as ARL_0) values 200 and 500, and three k values 0.25, 0.5, and 1. For each combination of ARL_0 and k, the corresponding value of h can be computed numerically using either the existing R-packages, such as the package spc, or a Monto Carlo simulation. The corresponding control charts are shown in Figure 5(a)–(c). From the plots, we can see that we have a convincing evidence of HFMD outbreaks around the 105th time point (i.e., March 16 2009) for all values of ARL_0 and k considered, and the evidence of HFMD outbreaks around the 91st time point (i.e., March 1 2009) is only marginally significant in cases when $k = 0.5$ and 1 and when $k = 0.25$ and $ARL_0 = 200$. For convenience of our perception, the two signaling time points $t = 91$ and $t = 105$ are plotted in the scatter plots of Y_t's and $\widehat{w}_t$'s by the vertical dashed lines in Figure 5(d)–(e). It can be seen that the CUSUM chart (4) can detect the HFMD outbreak in its early stage which is extremely helpful for us to take appropriate interventions early to prevent the widespread of the disease.

[Figure 5 about here.]

For the proposed three-step procedure described above, we evaluate its performance in terms of false positive rate (FPR) and false negative rate (FNR) in the next example. Because we do not really know the true status of disease outbreaks in real data, the following simulation study is performed instead. To mimic the HFMD data, in model (1), we consider the baseline function

$$f(t) = 0.05 + 0.05e^{-(t-150)^2/1000} + 0.001\cos\left(\frac{2\pi t}{365}\right) - 0.0005\sin\left(\frac{2\pi t}{365}\right), \text{ for } t = 1, 2, \ldots, 365,$$

and the error terms ε_t generated from the AR(1) model

$$\varepsilon_t = 0.0025\varepsilon_{t-1} + w_t, \qquad t \geqslant 1,$$

where w_t's are independent and identically distributed (i.i.d.) with the normal distribution $N(0, 0.75/200^2)$. To compute the FPR, we generate 365 observations from model (1) as IC data, and compute the local quadratic kernel estimate $\widehat{f}(t)$ and the estimated ARIMA model, as discussed in Sections 2.1 and 2.2. Then, another 365 observations are generated from model (1) as test data for sequential monitoring. After the first two steps of the proposed procedure (i.e., detrend and decorrelation) are applied to the test data, the CUSUM chart (4) with $ARL_0 = 500$ and $k = 0.25, 0.5$ or 1,0 is applied and it is recorded whether a signal is given when monitoring the test data. This process is then repeated 5,000 times, and the proportion of times that the CUSUM gives signals is used for estimating the FPR. For estimating the FNR, the simulation is performed in the same way, except that the test data are generated from model (1) in which the function $f(t)$ is replaced by $f(t) + \delta$, where

δ denotes a constant shift. In this study, we consider $\delta = 0.005, 0.01$, and 0.02. The results are presented in Table 1.

[Table 1 about here.]

From Table 1, it can be seen that the FNR's are quite small when $\delta = 0.01$ and 0.02, and they are relatively large when the shift is really small (i.e., $\delta = 0.005$). Regarding the FPR's, they are between 17-34%. Besides the parameter k, we find that the bandwidth parameter λ used in the local quadratic kernel estimation of $f(t)$ also has an impact on the FNR and FPR. To investigate this issue, besides the CV selection of λ, we also consider the cases when $\lambda = 0.1, 0.2, 0.3$, and 0.4. The results are shown in Figure 6. From plot (a), it can be seen that the FPR can be reduced a lot if we use a relatively large λ (e.g., $\lambda = 0.3$). In such cases, the FNR would also be quite small if the true shift is small (e.g., $\delta = 0.02$). So, in practice, if we prefer a relatively small FPR, then λ should be chosen a little larger than the value determined by the CV procedure.

[Figure 6 about here.]

3. Monitoring HFMD in Individual Provinces

In the previous section, we have demonstrated our proposed three-step procedure and used it for monitoring the HFMD data at the national level. This preliminary analysis shows that our method can detect the HFMD outbreak at an early stage. In practice, however, a warning of the HFMD outbreak at the national level has a limited influence on the decisions of local governments and local medical institutions regarding whether they should take some preventive measures (e.g., quarantine infected patients or reduce public gatherings) immediately after the national warning, since it is possible that only a few provinces are in the danger of an HFMD outbreak in such cases. If the number of reported HFMD cases remains relatively stable in a province, then such preventive measures would waste much public resource. On the other hand, if a province is under imminent threat of an HFMD outbreak, these preventive measures would be extremely important. Thus, it is necessary to monitor HFMD outbreaks at a local level. In this section, we geographically divide the HFMD data into thirty one groups, corresponding to the thirty one provinces in China, and apply the proposed method at the provincial level. The method, however, can also be used at a county or city level. The procedures for removing the seasonality and the temporal autocorrelation remain the same as those described in Section 2, except that M_t in (2) should be replaced by the population of each individual province. After using the ARIMA models to decorrelate the detrended data at the provincial level, the estimated parameters of the ARIMA models for individual provinces are listed Table 2. From the table, it can be seen that there is some difference among different provinces in regard to the temporal autocorrelation in the detrended data. But, the difference is quite small.

[Table 2 about here.]

However, our analysis shows that the distributions of the residuals of the fitted ARIMA models (i.e., the detrended and decorrelated data) are significantly different from normal distributions for most provinces. For instance, the histogram of the standardized residuals of the estimated ARIMA(0,1,1) model for the Hebei province is shown in Figure 7, together with the estimated density curve and the density curve of a standard normal distribution. From the plot, it can be seen that the distribution of the residuals is skewed to the right, and the Shapiro-Wilk normality test confirms that the distribution of the residuals is significantly different from a normal distribution. In such cases, the control limits of the conventional CUSUM chart (4) based on the normality assumption are invalid any more since the actual IC ARL values of the chart would be quite different from the pre-specified nominal IC ARL value in such cases (cf., Qiu and Hawkins, 2001; Qiu and Li 2011).

[Figure 7 about here.]

To overcome the difficulty due to the non-normality of the detrended and decorrelated data mentioned above, we suggest using the bootstrap procedure described below to search for the control limit of the CUSUM chart (4). Let $\mathcal{R}$ denote the set of the phase I detrended and decorrelated data of all 31 provinces. Then, $\mathcal{R}$ contains $80 \times 31 = 2480$ numbers since each province has 80 phase I detrended and decorrelated observations, as discussed in Section 2.2. Next, we randomly choose a sequence of numbers from $\mathcal{R}$ with replacement and the chosen numbers are denoted as $\{\widetilde{w}_t^*,\ t = 1, 2, \ldots\}$. For a given control limit $h^* > 0$, the run length (or signal time) is calculated by

$$RL_0^*(h^*) = \min_t \{t \geqslant 1, \quad C_t > h^*\},$$

where C_t is the same as that defined in (4) except that $\widehat{w}_t$ should be replaced by $\widetilde{w}_t^*$. The above step is repeated for $B = 50,000$ times, and B values of $RL_0^*(h^*)$ are obtained. Their averaged value is denoted as $ARL_0^*(h^*)$. Finally, we search for the h^* value such that $ARL_0^*(h^*)$ equals the pre-specified value of ARL_0. This h^* value is then used for monitoring the detrended and decorrelated data for individual provinces. In the case when $k = 0.25$ and $ARL_0 = 200$, the signal times of different provinces are presented in the map of Figure 8. The darker the color, the earlier the signal times. By this result, it seems that the HFMD outbreak starts from Beijing, the southern provinces Guangdong and Guangxi, and the mid-east provinces Henan and Shandong. It then spreaded to about a dozen provinces close to the east coast. A big region in the western and northern parts of China was not affected much by the HFMD outbreak. It can also be seen that the signal times of different province have some spatial correlation. Provinces that are geographically close to each other tend to have similar signal times of the HFMD outbreak. These results are quite consistent with some earlier studies (cf., Bie et al., 2010; Wang et al., 2011). The signal times of all 31 provinces in cases when $ARL_0 = 200$, or 500 and k = 0.25, 0.5, or 1 are summarized in Table 3. These results show that 1) the selection of ARL_0 and k has some impact on the signal time, but the impact is relatively small, and 2) the geographical pattern shown in the table matches with the geographical pattern in Figure 8 well. The only provinces in which the signal times are quite different when k changes are Yunnan and Gansu. After checking the data carefully, we found that the number of HFMD cases had a single-day jump in Yunnan on April 15, 2009, and it had a single-day jump in Gansu on April 13, 2009. In the literature, it has been well desmonstrated that CUSUM charts with a larger k will be more effective to detect transient shifts because the CUSUM charting statistic C_t defined in (4) uses less history data in such cases (i.e., it is reset to be 0 more often in the "max" operation in (4)). See Section 4.2 in Qiu (2014) for a detailed discussion. Therefore, the chart (4) can react to the single-day jump better when k is chosen larger. This explains why the signal times are shorter when k is chosen larger for Yunnan and Gansu in Table 3.

[Figure 8 about here.]

[Table 3 about here.]

For the above HFMD data, we also tried the sequential monitoring scheme by Marshall et al. (2007) that was based on the local Knox statistic proposed by Rogerson (2001), and the space-time scan method by Kulldorff (2001). Marshall et al. (2007) argued that their prospective monitoring scheme would be more effective than the original retrospective space-time method using the local Knox statistic. Their method assumed that the standardized disease incidence followed a normal distribution. The scan method, on the other hand, assumed that the disease incidence in a local region and within a time interval followed a Poisson distribution. In the HFMD example, the density histogram of the disease incidence in the Jilin province is shown in the left panel of Figure 9, where the solid and dashed curves denote the density curve of the data and the Poisson density with the same mean and standard deviation. It can be seen that the two curves are quite different. The Pearson's χ^2 test shows that the distribution of the disease incidence is significantly different from the

Poisson distribution with a p-value of 1.28×10^{-11}. The middle panel of Figure 9 shows the histogram of the standardized disease incidence, its density curve (solid), and the Normal density curve with the same mean and standard deviation (dashed). The Pearson's χ^2 test for checking whether the data follow a Normal distribution gives a p-value of 3.57×10^{-5}. We also found that the Poisson and Normal distributions were both invalid in all 31 provinces. Therefore, the existing methods based on these distribution assumptions are inappropriate to use in this example. Even if these distributional assumptions are pretended to be valid, performance of these methods is not good, as seen in the right panel of Figure 9 where the signal times of the CUSUM (4), scan, and local Knox methods are presented.

[Figure 9 about here.]

4. Concluding Remarks

We have proposed a three-step procedure to analyze the HFMD data obtained during December 2008 – November 2009 in China. The first two steps remove the seasonal trend and the temporal autocorrelation from the observed incidence rates, and the third step sequentially monitors the detrended and decorrelated data using a CUSUM chart. Our data analysis is performed at both the national level and the provincial level. A data-driven procedure is also suggested for obtaining the control limit of the CUSUM chart when it is used for monitoring the detrended and decorrelated data at the provincial level since the normality assumption required by the conventional CUSUM chart is found invalid in such cases. The numerical results presented in the paper show that our proposed method is capable to signal the HFMD outbreak at an early stage before the disease spreads to a large population. However, our current method still has some limitations. For instance, the possible spatial correlation in the observed HFMD data has not been fully accommodated in our data analysis. It requires much future research to develop effective methods for sequentially monitoring the spatio-temporal patterns of the disease incidence and for early detection and prevention of the disease outbreak.

5. Supplementary Materials

R codes implementing the proposed three-step procedure and the HFMD data analyzed in the paper are available with this paper at the Biometrics website on Wiley Online Library.

Acknowledgments: We thank the co-editor, Dr. Yi-Hau Chen, the associate editor, and two referees for their helpful comments and suggestions, which greatly improved the quality of the paper. This research is supported in part by an NSF grant.

References

Bie, Q., Qiu, D., Hu, H., and Ju, B. (2010), "Spatial and temporal distribution characteristics of hand-foot-mouth disease in china," *Journal of Geo-Information Science*, **12**, 380–384.

Box, G. E., and Jenkins, G. M. (1976), *Time series analysis, control, and forecasting,* San Francisco, CA: Holden Day.

Dickey, D.A., and Fuller, W.A. (1979), "Distribution of the estimators for autoregressive time series with a unit root," *Journal of the American Statistical Association*, **74**, 427–431.

Jiang, W., Han, S. W., Tsui, K.-L., and Woodall, W. H. (2011), "Spatiotemporal surveillance methods in the presence of spatial correlation," *Statistics in Medicine*, **30**, 569–583.

Jiang, W., Tsui, K.L., and Woodall, W. (2000), "A new SPC monitoring method: the ARMA chart," *Technometrics*, **42**, 399–410.

Kwiatkowski, D., Phillips, P. C., Schmidt, P., and Shin, Y. (1992), "Testing the null hypothesis of stationarity against the alternative of a unit root: How sure are we that economic time series have a unit root?" *Journal of Econometrics*, **54**, 159–178.

Kulldorff, M. (2001), “Prospective time periodic geographical disease surveillance using a scan statistic,” *Journal of the Royal Statistical Society (Series A)*, **164**, 61–72.

Lin, X., and Carroll, R. J. (2000), “Nonparametric function estimation for clustered data when the predictor is measured without/with error,” *Journal of the American Statistical Association*, **95**, 520–534.

Lu, C.W., and Reynolds, M.R., Jr. (2001), “Control charts for monitoring an autocorrelated process,” *Journal of Quality Technology*, **33**, 316–334.

Maragah, H.D., and Woodall, W.H. (1992), “The effect of autocorrelation on the retrospective x-chart.,” *Journal of Statistical Computation and Simulation*, **40**, 29–42.

Marshall, J.B., Spitzner, D.J., and Woodall, W.H. (2007), “Use of the local Knox statistic for the prospective monitoring of disease occurrences in space and time,” *Statistics in Medicine*, **26**, 1579–1593.

Montgomery, D., Mastrangelo, C., Faltin, F. W., Woodall, W. H., MacGregor, J. F., and Ryan, T. P. (1991), “Some statistical process control methods for autocorrelated data,” *Journal of Quality Technology*, **23**, 179–204.

Moustakides, G. V. (2004), “Optimality of the cusum procedure in continuous time,” *The Annals of Statistics*, **32**, 302–315.

Qiu, P. (2005), *Image Processing and Jump Regression Analysis,* New York: John Wiley & Sons.

Qiu, P. (2014), *Introduction to statistical process control,* Boca Raton, FL: Chapman and Hall/CRC Press.

Qiu, P., and Hawkins, D. (2001), “A rank based multivariate CUSUM procedure,” *Technometrics*, **43**, 120–132.

Qiu, P., and Li, Z. (2011), “On nonparametric statistical process control of univariate processes,” *Technometrics*, **53**, 390–405.

Rogerson, P.A. (2001), "Monitoring point patterns for the development of space-time clusters," *Journal of the Royal Statistical Society (Series A)*, **164**, 87–96.

Rogerson, P. A., and Yamada, I. (2004), "Monitoring change in spatial patterns of disease: comparing univariate and multivariate cumulative sum approaches," *Statistics in Medicine*, **23**, 2195–2214.

Shumway, R. H. and Stoffer, D. S. (2011), *Time series analysis and its applications: with R examples,* New York: Springer.

Wang, Y., Feng, Z., Yang, Y., Self, S., Gao, Y., Longini, I. M., Wakefield, J., Zhang, J., Wang, L., Chen, X., Yao, L., Stanaway, J. D., Wang, Z., and Yang, W. (2011), "Hand, foot, and mouth disease in china: patterns of spread and transmissibility," *Epidemiology*, **22**, 781–792.

Watier, L., Richardson, S., and Hubert, B. (1991), "A time series construction of an alert threshold with application to s. bovismorbificans in france," *Statistics in Medicine*, **10**, 1493–1509.

Williamson, G. D., and Hudson, G. W. (1999), "A monitoring system for detecting aberrations in public health surveillance reports," *Statistics in Medicine*, **18**, 3283–3298.

Woodall, W. H. (2006), "The use of control charts in health-care and public-health surveillance," *Journal of Quality Technology*, **38**, 89–104.

World Health Organization (2011), "A guide to clinical management and public health response for hand, foot, and mouth disease (HFMD)," *World Health Organization Report.*

Zhou, H., and Lawson, A. B. (2008), "EWMA smoothing and Bayesian spatial modeling for health surveillance," *Statistics in Medicine*, **27**, 5907–5928.

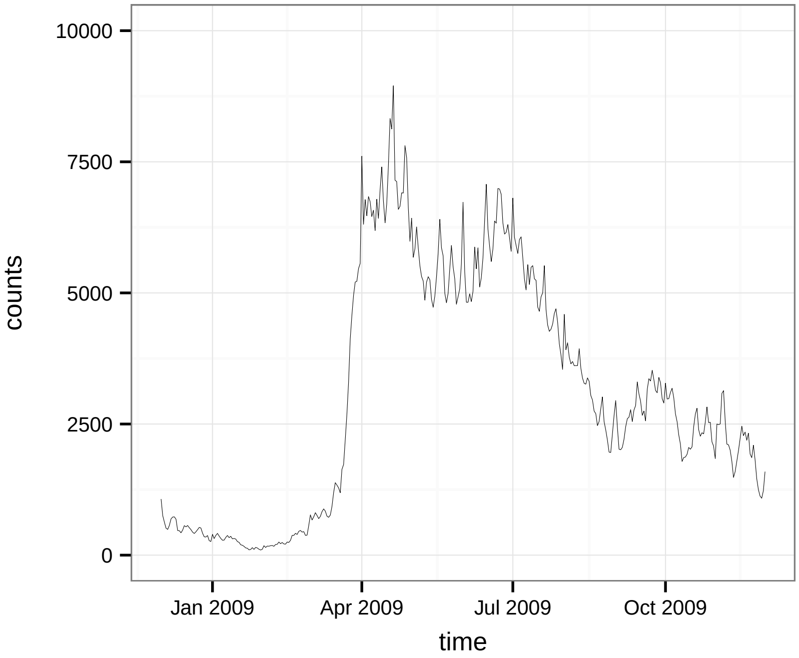

Figure 1: Observed daily incidences of the Hand, Foot and Mouth Disease in China during December 2008 and November 2009.

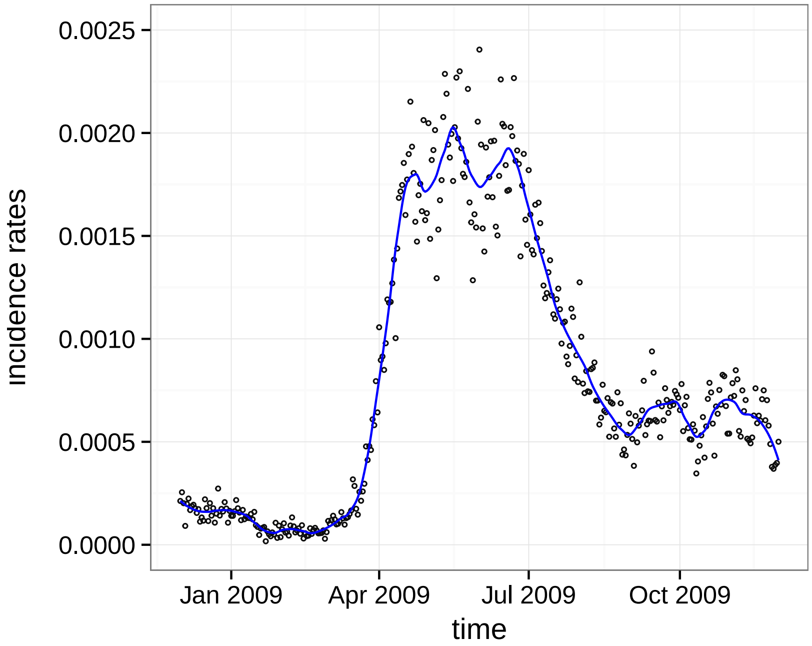

Figure 2: Solid line denotes $\widehat{f}(t)$, and little circles denote the averaged daily incidence rates of the five provinces included in the baseline data.

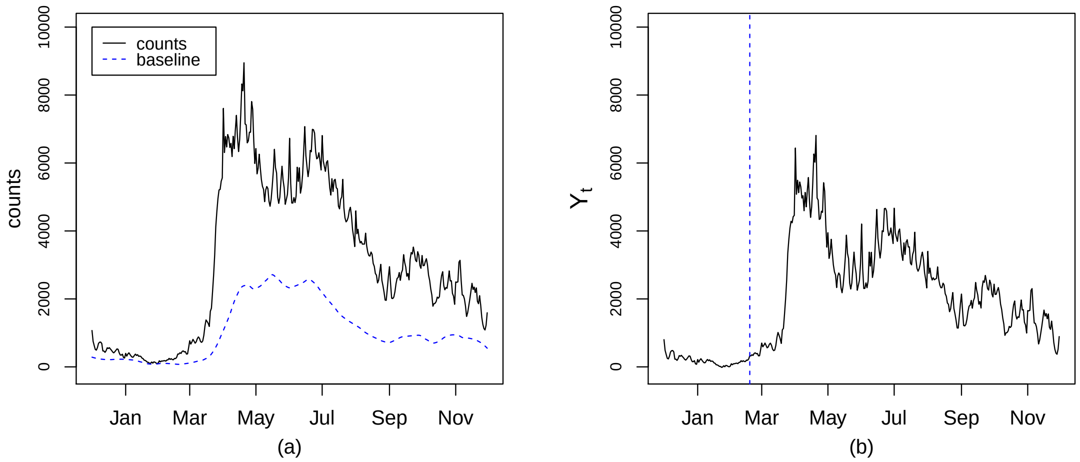

Figure 3: (a): The solid and dashed lines denote the observed daily counts Z_t of HFMD and the estimated baseline daily counts $\widehat{f}(t)M_t$. (b): The solid line denotes the detrended data Y_t, and the dashed vertical line separates the first 80 observations from the remaining ones.

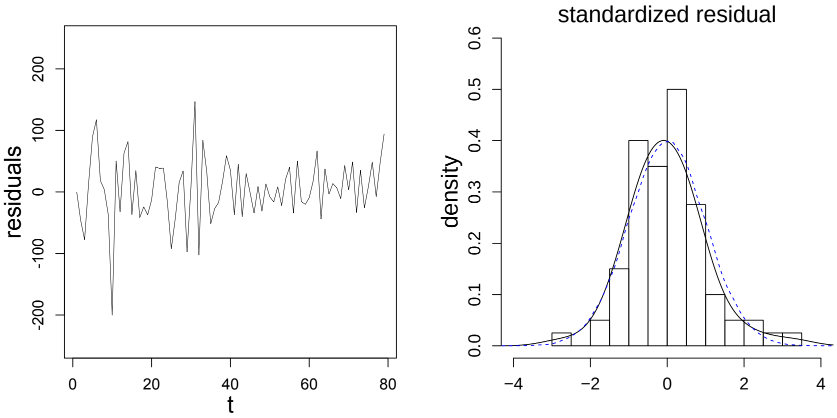

(a)

(b)

Figure 4: (a): Residual plot of the model (3) for the first 80 observations. (b): Density histogram of the residuals shown in (a), the corresponding estimated density curve (solid), and the density curve of the normal distribution with the same mean and variance (dashed).

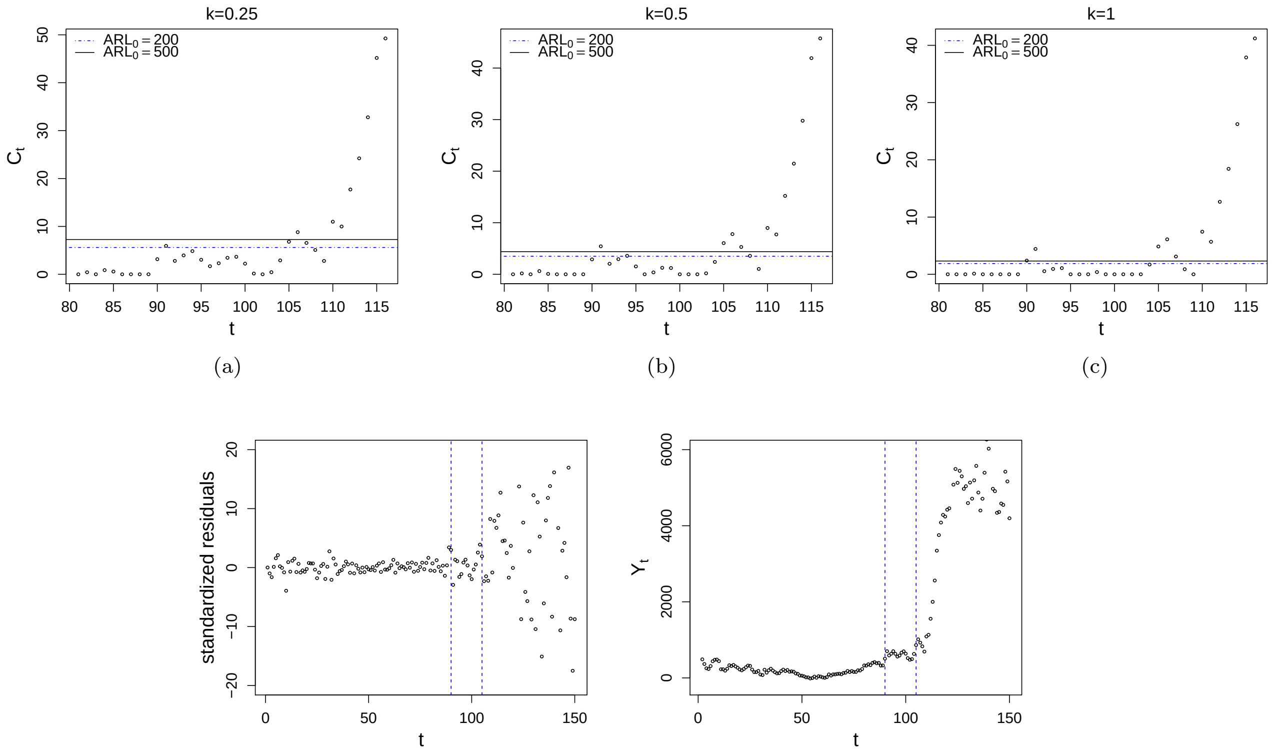

(a) (b) (c)

(d) (e)

Figure 5: (a)-(c): CUSUM charts when $k = 0.25$, 0.5 and 1, respectively. The horizontal dot-dashed and solid lines denote the control limits when $\mathrm{ARL}_0 = 200$ and 500, respectively. (d)-(e): Scatter plots of Y_t's and $\widehat{w}_t$'s with the vertical dashed lines denoting the signaling time points $t = 91$ and $t = 105$.

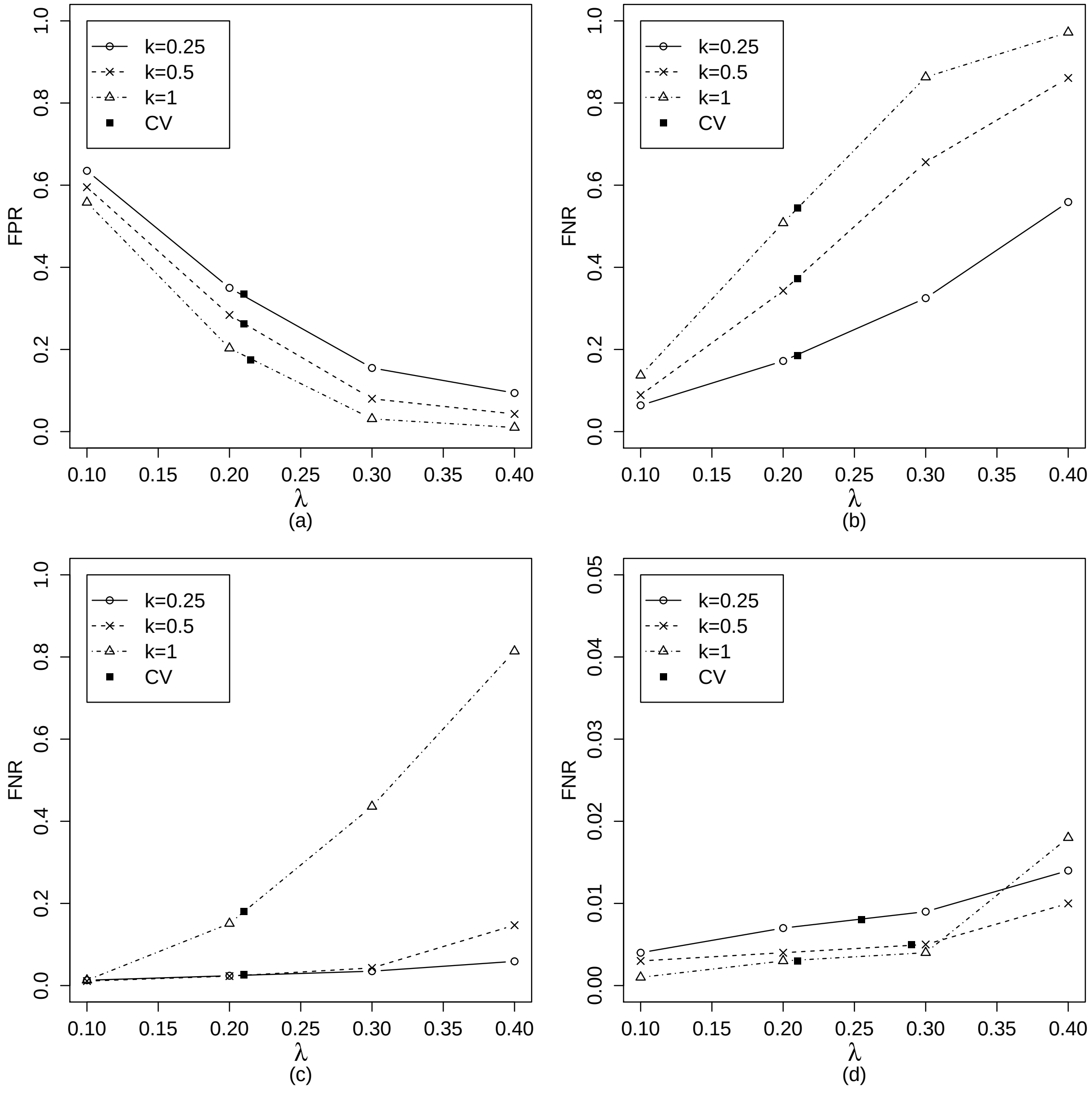

Figure 6: Estimated FPR's (plot (a)) and estimated FNR's when $\delta = 0.005$ (plot (b)), 0.01 (plot (c)), and 0.02 (plot (d)). In this example, $k = 0.25, 0.5, 0.1$ and $\lambda = 0.1, 0.2, 0.3, 0.4$. The dark points in each plot show the FPR's and FNR's when λ is chosen by the 10-fold CV procedure. Note that the y-axis scale in plot (d) is different from those of the other three plots.

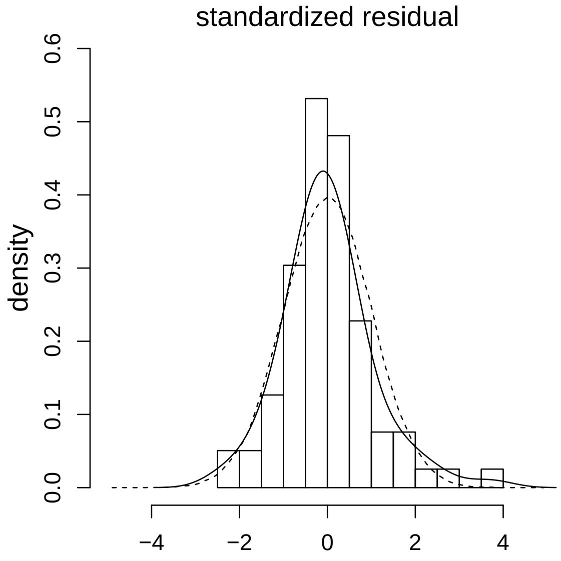

Figure 7: Density histogram of the standardized residuals of the estimated ARIMA model for the Hubei province, the estimated density curve (solid line), and the density curve of the standard normal distribution (dashed line).

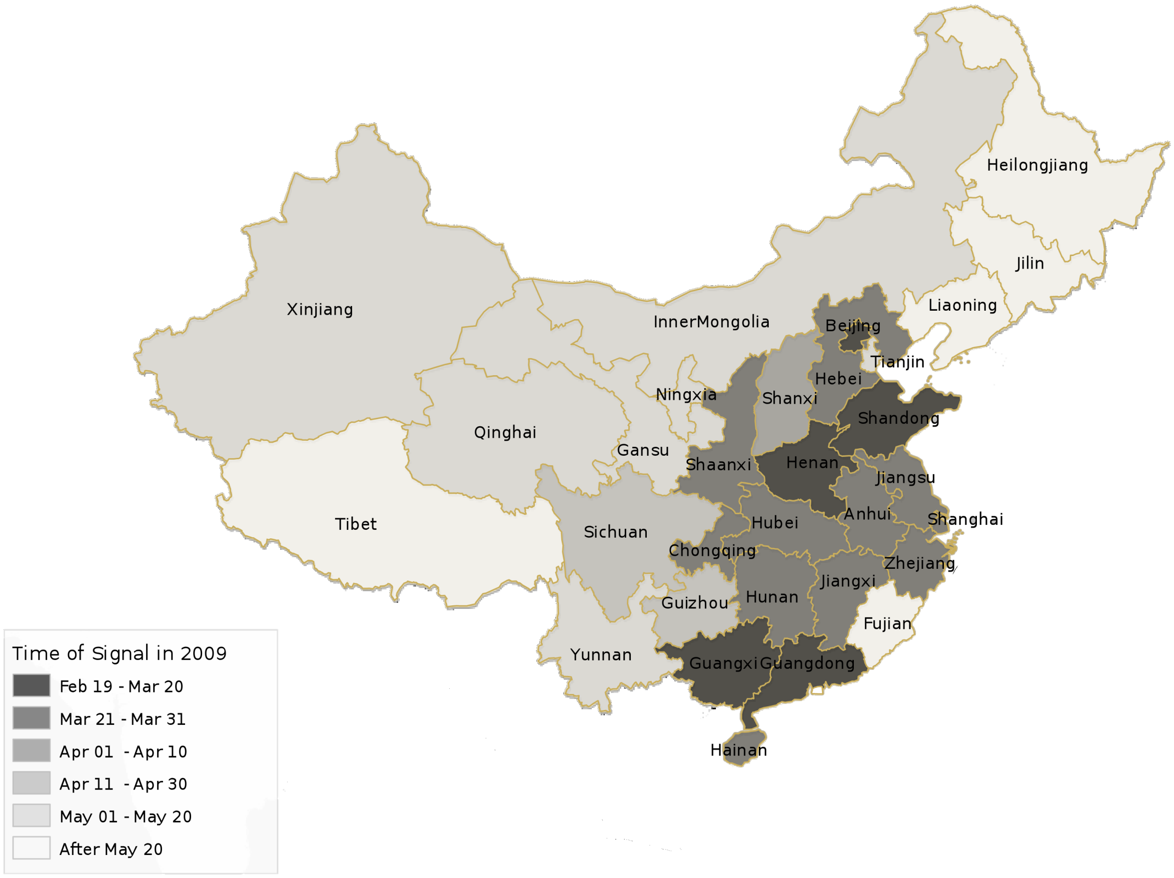

Figure 8: Signal times of the 31 provinces in China about the HFMD outbreak in 2009. The darker the colors, the earlier the signal times.

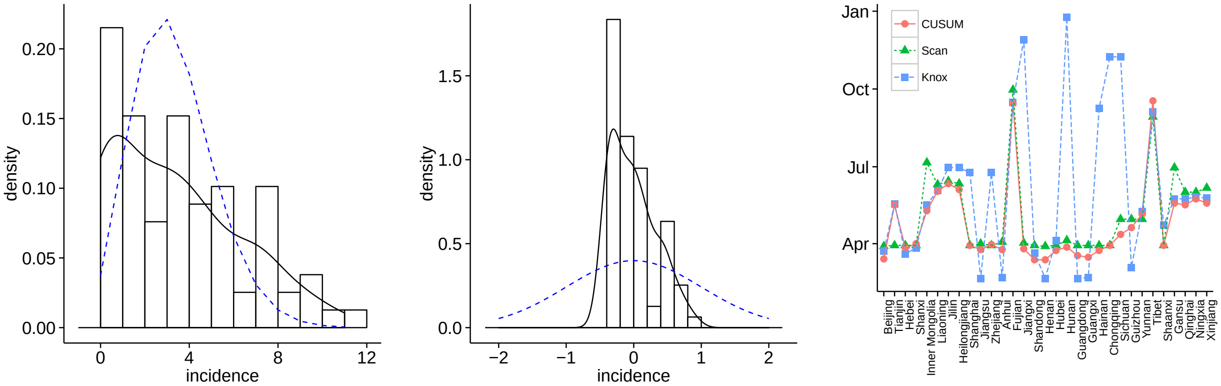

Figure 9: Left panel: Density histogram and curve (solid) of the HFMD incidences in the Jilin province, and a Poisson density (dashed) with the same mean and standard deviation. Middle panel: Same as left panel, except that it is for the standardized HFMD incidences and the dashed curve is a Normal density. Right panel: Signal times of the CUCUM (4), scan, and Knox methods for monitoring the reported HFMD incidences in 31 provinces of China.

Table 1: Simulation results about the FPR (the first row with $\delta = 0$) and the FNR (the remaining rows) of the proposed three-step procedure based on 5,000 replications. Numbers in parentheses are the standard errors in the unit of 10^{-3}. The 10-fold CV procedure is used for choosing the bandwidth parameter when estimating the baseline function $f(t)$.

δ	$k = 0.25$	0.5	1.0
0	0.335 (4.203)	0.262 (4.080)	0.175 (3.553)
0.005	0.185 (2.786)	0.372 (4.579)	0.545 (5.775)
0.01	0.026 (0.286)	0.027 (0.408)	0.180 (3.202)
0.02	0.008 (0.057)	0.005 (0.056)	0.003 (0.069)

Table 2: Estimated parameters of the ARIMA models for individual provinces.

	Province	p	d	q		Province	p	d	q
1	Beijing	0	1	1	17	Hubei	1	1	1
2	Tianjing	2	1	1	18	Hunan	1	1	1
3	Hebei	0	1	1	19	Guangdong	1	0	1
4	Shanxi	0	1	1	20	Guangxi	1	1	1
5	Inner Mongolia	0	1	1	21	Hainan	0	1	1
6	Liaoning	2	1	2	22	Chongqing	0	1	1
7	Jilin	1	1	2	23	Sichuan	0	0	0
8	Heilongjiang	0	1	2	24	Guizhou	2	1	2
9	Shanghai	1	1	1	25	Yunan	1	0	1
10	Jiangsu	1	1	1	26	Tibet	0	1	1
11	Zhejiang	1	0	0	27	Shaanxi	1	1	1
12	Anhui	1	1	1	28	Gansu	0	1	1
13	Fujian	1	1	1	29	Qinghai	0	1	1
14	Jiangxi	0	1	1	30	Ningxia	1	1	2
15	Shandong	1	1	1	31	Xinjiang	2	1	1
16	Henan	0	1	1					

Table 3: Signal times of all 31 provinces obtained from the CUSUM chart (4) when ARL_0 = 200, or 500, and k = 0.25, 0.5, or 1.

Province	$ARL_0 = 200$			$ARL_0 = 500$		
	k=0.25	k=0.5	k=1	k=0.25	k=0.5	k=1
Beijing	22	23	24	24	24	25
Tianjin	88	86	86	88	88	88
Hebei	36	37	37	37	37	37
Shanxi	41	41	61	43	42	61
Inner Mongolia	80	80	81	81	81	81
Liaoning	102	107	114	107	104	106
Jilin	107	112	114	114	113	114
Heilongjiang	106	106	106	106	106	106
Shanghai	39	39	39	41	40	41
Jiangsu	34	34	34	35	35	34
Zhejiang	37	40	43	40	41	43
Anhui	34	34	34	35	35	34
Fujian	208	208	208	208	208	208
Jiangxi	36	36	36	36	36	36
Shandong	23	22	23	24	23	23
Henan	23	22	22	23	23	23
Hubei	34	34	34	34	34	34
Hunan	37	37	37	38	38	38
Guangdong	28	28	28	29	28	28
Guangxi	23	20	26	26	26	26
Hainan	33	34	34	34	34	34
Chongqing	40	39	39	40	40	39
Sichuan	53	53	42	53	53	53
Guizhou	51	61	61	61	61	61
Yunnan	77	56	56	83	77	56
Tibet	211	211	211	212	211	211
Shaanxi	40	40	40	40	40	40
Gansu	91	54	54	91	90	54
Qinghai	88	88	88	89	88	88
Ningxia	91	91	95	95	95	95
Xinjiang	90	90	90	90	90	90